Original Research Article

International Journal of
Protective Structures

Ballistic performance of Armox500T and Hardox450 double-layered steel plates under 7.62×51 mm FMJ bullet impact

International Journal of Protective Structures
2025, Vol. 0(0) 1–18

DOI: 10.1177/20414196251391439
journals.sagepub.com/home/prs
Sage

Mehmet Özer[1], Fatih Balıkoğlu[1] and İbrahim Kutay Yılmazçoban[2]

Abstract

This work performed a nonlinear numerical analysis of Armox 500T and Hardox 450 armour steels, under ballistic conditions, validating the results via experimental data. The ballistic performance of seven distinct armour configurations were investigated, including monolithic, and double-layered armour steels. Ballistics tests were conducted using 7.62 full metal jacket bullets with a muzzle velocity of 837 ± 3.08 m/s, under the NIJ 0108.01 III protection level standard. Monolithic Armox 500T steel exhibited superiority over double-layer Armox 500T and Hardox 450 steels with regard to ballistic protection, weight, and cost-effectiveness. The fully perforated monolithic Armox 500T steel plate exhibited a reduced bullet exit velocity compared to Hardox 450 steel and produced a smaller exit hole for the bullet. Comprehensive finite element simulations of the ballistic impact events were conducted to elucidate the phenomena of defeat and penetration with greater precision.

Keywords

armour, ballistic impact, double-layered steel, finite element, damage

Introduction

Developing the ability to withstand high-calibre bullets and reduce weight is a crucial objective for applications in the military. Hardened steel plates are frequently employed as armour against the ballistic threat of rifle bullets and fragments with similar destructive power. This can be characterized

[1]Faculty of Engineering, Department of Mechanical Engineering, Balıkesir University, Çağış Yerleşkesi, Altıeylül/Balıkesir, Turkey
[2]Faculty of Engineering, Department of Mechanical Engineering, Sakarya University, Esentepe Kampüsü, Serdivan/Sakarya, Turkey

Corresponding author:
Fatih Balıkoğlu, Faculty of Engineering, Department of Mechanical Engineering, Balıkesir University, Çağış Yerleşkesi, 10145 Altıeylül/Balıkesir, Turkey.
Email: fatih.balikoglu@balikesir.edu.tr

by steels that exhibit high ductility, as well as high hardness and strength values. In addition to these attributes, it is crucial to consider its superior loading capacity, inexpensive price compared to most other armour materials, and its ease of shaping. Even though monolithic steel plates are manufactured in extremely thick thicknesses to meet commercial demands, the utilization of thin steel plates is more advantageous in armour applications in terms of maintenance and mobility (Børvik et al., 2003; Børvik, Hopperstad, et al., 2002; Børvik, Langseth, et al., 2002; Qiang et al., 2022). In addition, the multi-layered design of thin steel armour sheets provides users with more flexibility for maintenance and mobility. Therefore, instead of monolithic plates, most numerical and experimental investigations on steel plate ballistic performance employ layered plates of the same thickness (İbış et al., 2023; Orlov et al., 2024; Orlov and Fazylov, 2022; Ranaweera et al., 2020). These studies aimed to minimize armour plate weight while preserving ballistic protection comparable to monolithic steel sheets.

The ballistic performances of laminated steel armours have been studied in detail in the literature. Senthil and Iqbal (Senthil and Iqbal, 2021) investigated the ballistic performance of layered configurations of Armox 500T, mild steel, and Al 7075-T651 sheets against 7.62 AP bullets in normal and oblique shots. As the best configuration, authors suggested to use low ductility-high strength Armox 500T in the upper layer, and high ductility-low strength Al 7075-T651 or medium strength-medium ductile mild steel in the middle layer and bottom layer. Paman et al. (Paman et al., 2020) studied the optimal order and thickness of the material layers of a multi-layered armour module by numerical simulation and ballistic experiments to provide both ballistic resistance against 7.62 armour-piercing bullets and minimum weight. Paman et al. demonstrated the methodology by applying it to three metal alloys: Armox-500T, Ti-6Al-4V, and Al-2024. They first carried out numerical simulations to examine the ballistic impact behaviour of these three materials using the AUTODYN-3D code. Ballistic experiments showed that the Armox-500T/Ti-6Al-4 V/Al-2024 array, with 5.5, 8.5 and 13 mm thicknesses, respectively, has the best resistance against 7.62 mm armour-piercing bullets. It was found that the composite module was more efficient than Armox-500T and Al-2024 in terms of weight and had better performance than Al-2024 in terms of armour thickness. Acar D. et al. (Acar et al., 2024) investigated the ballistic impact response of Armox Advance, Ramor 500, and Hardox 450 steels with monolithic, double-layer, and perforated plate configuration against 7.62 mm NATO Cannon, 7.62 × 51 AP, and 12.7 mm APM2 bullet threats. Double-layer plate combinations consisting of a 10 mm thick Armox Advance back plate and either a 5 mm or 6.5 mm Ramor 500 front layer plate or a 6 mm Hardox 450 front layer plate provide complete ballistic protection against 7.62 mm AP bullets. Bekci et al. (Bekci et al., 2021) experimentally and numerically examined the ballistic performances of Ramor 500 and Ramor 550 armour steel plates against 7.62 mm bullets under various conditions. Three different configurations were used in the experimental study: monolithic plate, double-layer plate, and bent plate. The 6.7 mm thick Ramor 500 and 6.2 mm thick Ramor 550 monolithic plates failed the tests the structure with Ramor 550 as the face plate showed better ballistic resistance in double-layer test plates. It was also reported that the ballistic resistance of the plates increases as the impact angle increases.

The objective of this study is to evaluate whether the NIJ 0108.01 Level III protection requirement for light armoured vehicles can be satisfied by replacing monolithic Armox 500T steel armour plates with double-layered steel plates This study aimed to provide protection against 7.62 × 51 mm full metal jacket (FMJ) bullets with a speed of 837 ± 3.08 m/s. Additionaly, this study contributed to the literature by evaluating the ballistic performance of high wear resistant Hardox 450 steel, which may be used to replace costly armor Armox 500T steel. Firstly, the finite element model of the target steel plates including material modelling was prepared in LS Dyna® software. A

parametric analysis was performed by evaluating the ballistic testing of seven steel plate designs with different thicknesses and layer arrangements; the perforation event, back face deformation and failure mechanisms were compared to the experimental results. The ballistic protection, weight, and cost performance of double-layered structures using 8 mm thick Armox 500T and Hardox 450 steels were compared to those of 6 mm thick Armox 500T armor steel.

Materials and methods

Armour materials

A parametric study with seven different armour plate configurations was conducted to determine whether the targets produced within the scope of the study fulfil the protection level specified in the NIJ STD-0108.01 Level III standard (NIJ 0108.01, 1985). The steel layers used in all configurations are made of Armox 500T and Hardox 450 steel. The chemical compositions of the two steels from the SSAB firm are presented in (Table 1), and their mechanical properties are detailed in (Table 2). The configuration of all armour plates included in the experimental study is illustrated in (Table 3). The letters "A" and "H" in the sample abbreviations refer to Armox500T and Hardox450 steel plates respectively. As seen in Table 3, the k number represents the cost of one square meter of 4 mm Hardox450 steel. Steel prices were determined using the current euro exchange rate as of December 16, 2024.

Full metal jacket bullet

According to NIJ STD-0108.01 Level III, 7.62 × 51 mm NATO FMJ bullet was selected with a speed standard of 837 ± 3.08 m/s. All residual velocity of core after full perforation values were recorded and compared in the parametric study. (Figure 1) illustrates the 7.62 × 51 mm FMJ projectile utilized in the parametric investigation, whereas (Table 4) indicates the characteristics of the 7.62 × 51 mm FMJ bullet.

Ballistics test

Ballistics tests were conducted in the indoor shooting range of ZSR corporation located in Balikesir province, Türkiye. The closed range had an air conditioning system, and the ambient temperature was maintained at 22°C during the experiments. This ambient temperature falls between the 20-28°C range specified in the standard. Armor plate targets were hit with the Prototypa brand gun in (Figure 2(a)) in this range, utilizing the 7.62 × 51 mm calibre FMJ bullet manufactured by this company. To measure the muzzle velocity of the bullets, five test shots were shot in a closed range without a target plate, producing an average of 837 m/s and a standard deviation of 3.08 m/s. The ballistic test setup was set at level III protection within the scope of the "NIJ 0108.01 Ballistic

Table 1. The amount of alloying elements in Armox 500T and Hardox 450 steels (Armox 500T General Product Description, 2016).

Elements	C	Si	Mn	P	S	Cr	Ni	Mo	B
Armox 500T	0.32%	0.4%	1.2%	0.015%	0.010%	1.01%	1.18%	0.7%	0.005%
Hardox 450	0.26%	0.7%	1.6%	0.025%	0.010%	1.40%	1.50%	0.5%	0.005%

Table 2. Mechanical properties of Armox 500T and Hardox 450 steels (Armox 500T General Product Description, 2016).

Properties	Symbols	Unit	Armox 500T	Hardox 450
Hardness	*HBW*	–	480-540	420-475
Impact toughness at −40°C (Charpy)	*KV*	J	32	35
Yield strength	$R_{p0,2}$	MPa	1250	1200
Ultimate strength	R_m	MPa	1450-1750	1400

Note: A5 (extensometer range of 5 mm), A50 (extensometer range of 50 mm).

Resistant Protective Materials" standard (Figure 2(b)). Five shots were completed on the test plates in compliance with the standard. A single comprehensive photograph illustrating the damage caused by the bullets on the plate was identified, and the damage status of the relevant plate was shown during the experiments. Double-layered steel plates were placed in order in the test setup, with no adhesive used. The plates have been fixed by placing them in a frame with four sides. The target plates were supported without using clay in accordance with the standard (Figure 2(c)). The distance between the test plate and the gun barrel was set as 15 m at protection level III. In ballistic laboratory tests, bullet exit velocities were not measured due to the risk of being detrimental to ZSR's velocity measuring apparatus; just muzzle exit velocities were recorded. The exit velocity values obtained from finite element analyses are presented in this study.

Finite Element (FE) modelling

Mesh procedure. Initially, a CAD model of the ammunition was made by utilizing measurements from an actual 7.62 × 51 mm FMJ bullet. Half of the bullet was meshed using eight-node brick elements with limited integration (Element Formulation, Type 1) and stiffness-based hourglass control. The mesh structure of the projectile-armour elements was created manually within the LS-DYNA® Suite's LS-PrePostsoftare. The numerical model included 89,635 elements for the 7.62 mm FMJ projectile, with mesh diameters varying from 0.07 to 0.25 mm. The bullet's striking location to the armour plate is where the penetration occurs; hence, it is represented by a finer mesh structure. A half model was created for each target using the same element type as the bullet. The mesh sizes in the target plate were assigned between 0.25 and 0.625 mm This modelling technique aims to minimize processing time needs while maintaining an optimal system balance. Then it was revolved to form a completely solid mesh. For Armox 500T and HARDOX 450 steels,

Table 3. Target plates configurations.

Configuration	Geometry	Code	Total thickness (mm)	Layers	Areal density ρ_A (kg/m^2)	Cost/m^2
Monolithic steels		4A	4	1 × 4 mm steel	7.83	2.02k
		4H	4	1 × 4 mm steel	8.13	k
		6A	6	1 × 6 mm steel	7.83	3.02k
		6H	6	1 × 6 mm steel	8.13	1.50k
Double-layered steels		4A4H	8	2 × 4 mm steel	7.98	3.02k
		4H4A	8	2 × 4 mm steel	7.98	3.02k
		4H4H	8	2 × 4 mm steel	8.13	2k

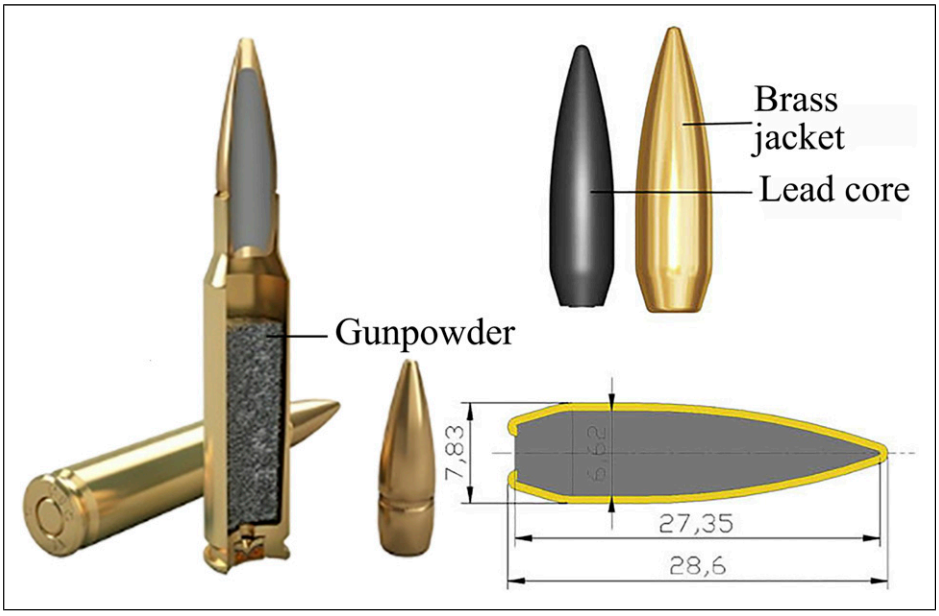

Figure 1. 7.62 × 51 mm FMJ bullet and dimensions used in the experimental and numerical study.

276,480 elements were defined. Figure 3 shows the boundary condition where the armour plates remain fixed at each degree of freedom along their four side surfaces.

Two simulations were conducted on the 6 mm Armox 500T test using a system including an Intel Core i9-12,900 KF CPU and 64 GB of RAM with LS-DYNA® Solver using 8 MPP cores to ascertain the appropriate element size. The simulations utilized element sizes of 0.5 mm and 0.25 mm for all components. While the contact relation parameters were held constant, the contact stiffness and contact time-step were adjusted in accordance with the element size. Comparative analysis of the simulation results with experimental data revealed that the 0.5 mm element size reduced the solution time by a factor of 16. However, this efficiency came at the expense of accuracy, with the deformation value on the targets back surface being 14.7% higher than the experimental result. In contrast, the 0.25 mm element size, despite requiring a longer computational time, produced results that were in closer agreement with the experimental data, exhibiting a back deformation depth that was 6.1% lower. The mesh size for the target plate is consistent with previous findings in the literature (Morghode et al., 2024a; 2024b).

Table 4. Technical specifications of 7.62 × 51 mm FMJ ammunition.

Bullet	7.62 mm FMJ
Core diameter	7.83 mm
Core weight	9.60 g
Cartridge case weight	11.84 g
Length	28.6 mm
Gunpowder quantity	2.768 ± 0.005 g
Average velocity	837 m/s

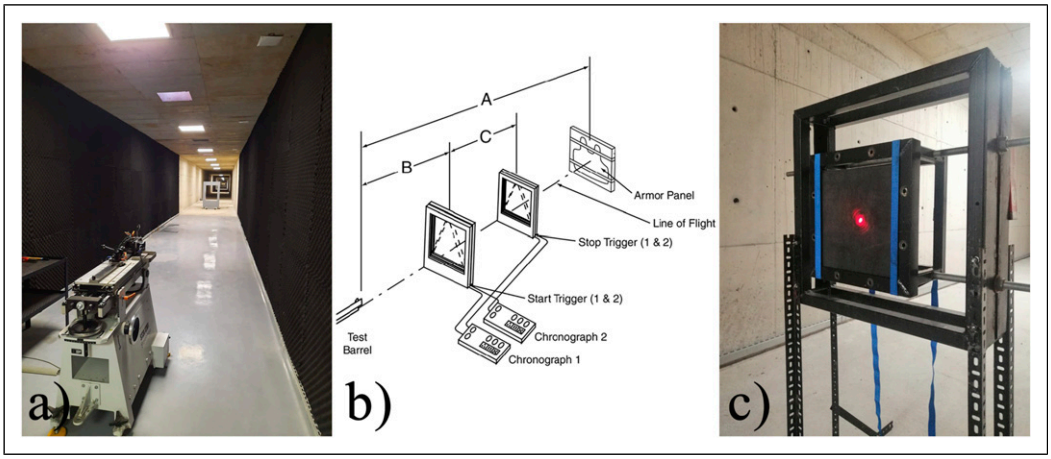

Figure 2. (a) Closed range and prototype brand shooting apparatus belonging to ZSR A.Ş. Company; (b) schematic view of the test standard (NIJ STD-0108.01 level III) (NIJ 0108.01, 1985); (c) target plate holder.

Material model. The MAT_015_JOHNSON_COOK (Mubashar et al., 2019; Mulabagal et al., 2024) material model was used for the steels because of its excellent precision and stable performance, not affected by dynamic fluctuations in deformation rate for explicit dynamic conditions. This material model includes the effects of temperature, strain rate, and strain hardening (Johnson GR., 1983; Sirigiri et al., 2022). The material model of Armox 500T was obtained from literatüre (Saleh, 2016).

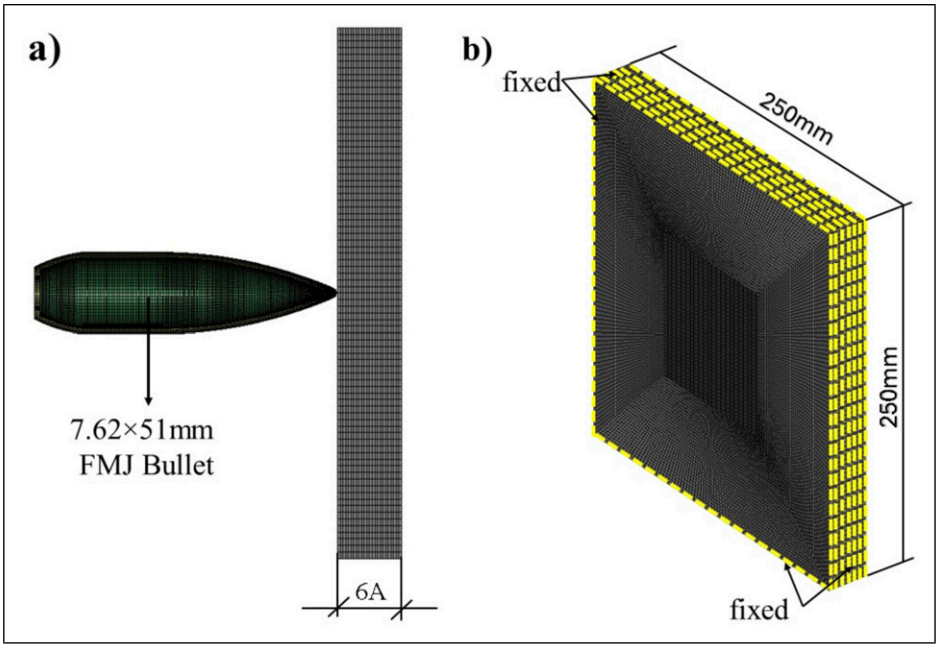

Figure 3. Details of the finite element model (a) Sectional view of the finite element model of the 6A armour steel plate (b) Image of the zero-degree-of-freedom points of the armour plate.

Table 5. Material properties for Armox 500T (Saleh, 2016) and Hardox 450 armor steels.

Mechanical properties	Hardox 450	Armox 500T
Density, ρ (Kg/mm^3)	8.13E-06	7.83E-06
Shear modulus, G (GPA)	71.80	79.60
Yield stress, A (GPA)	1.0690	0.3850
Hardening constant, B (GPA)	0.9371	1.4050
Hardening exponent n	0.3438	0.0263
Strain-rate sensitivity constant, c	0.0911	0.0870
Temperature sensitivity exponent, m	1.0000	1.0440
Failure parameters		
D1	1.6900	0.0680
D2	−0.2843	5.3280
D3	−0.1837	2.5540
D4	0.0600	0.0000
D5	0.0000	0.0000

As for Hardox 450, Johnson-Cook parameters for behaviour were calculated following equations (1) and (2) (Kasilingam et al., 2019; Miloradovic et al., 2025; Senthil et al., 2015)

$$\sigma_y = (A + B\varepsilon^n)(1 + \mathrm{C}\ln(\dot{\varepsilon}^*))(1 - T^{*m}) \tag{1}$$

where; σ_y is the flow of stress, A is the yield strength, B is the strain hardening modulus, ε is the equivalent plastic strain, n is the strain hardening exponent, C is the strain rate sensitivity coefficient and m is the thermal softening. $\dot{\varepsilon}^*$ represent the dimensionless strain rate T^* is the homologous temperature.

For the fail parameters;

$$e^f = (D_1 + D_2\exp(D_3\sigma^*))(1 + D_4\ln\acute{\varepsilon}^*)(1 + D_5T^*) \tag{2}$$

where, e^f is the strain at fracture, D1 to D5 is the constants, σ* is the ratio of mean stress divided by equilavent stress (stress triaxiality).

To calculate the necessary material parameters, since material parameters weren't found in the literature, tensile test data from Ulewicz et al. (2013) was used because tensile testing was not available to the researchers at the time of the study due to a malfunction of the required apparatus. Table 5 displays the material properties of Armox 500T20 and Hardox 450 armour steel plates.

Numerical stability and contact assignments. To address the challenges presented by the high velocity of the bullet, several adjustments were made to the contact algorithms and numerical controls to

Table 6. Details of the control assignments.

Card changed	Parameter changed	Value
CONTROL_TIMESTEP	TSSFAC	0.85
CONTROL_ENERGY	HGEN	1
CONTROL_CONTACT	ECDT	1

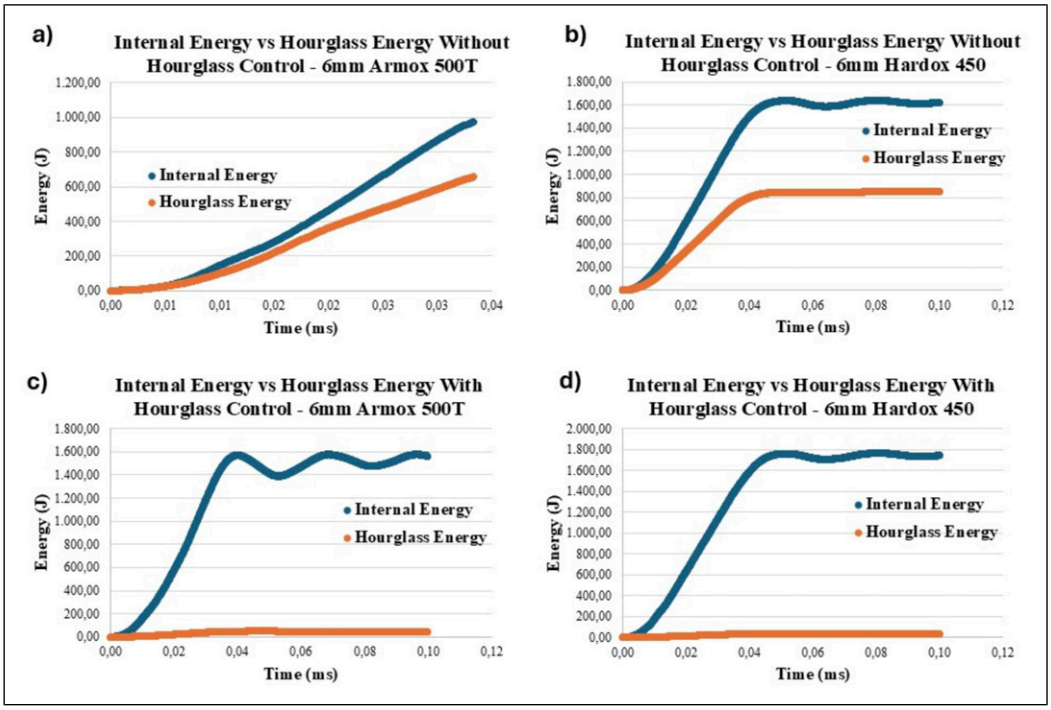

Figure 4. Comparison of internal and hourglass energy time graphs.

ensure both accuracy and computational efficiency. The CONTROL_TIMESTEP card's timestep scale factor was set to 0.85 to optimize the analysis and contact relationships as with the default value of 0.9 contact would fail to detect. Additionally, the HOURGLASS energy option was activated within the CONTROL_ENERGY card (option HGEN) to monitor hourglass energies (Table 6). Initial simulations without hourglass controls for the targets showed unacceptably high hourglass energies to the point of 6 mm thick Armox 500T being unsolvable by the solver giving out a direct

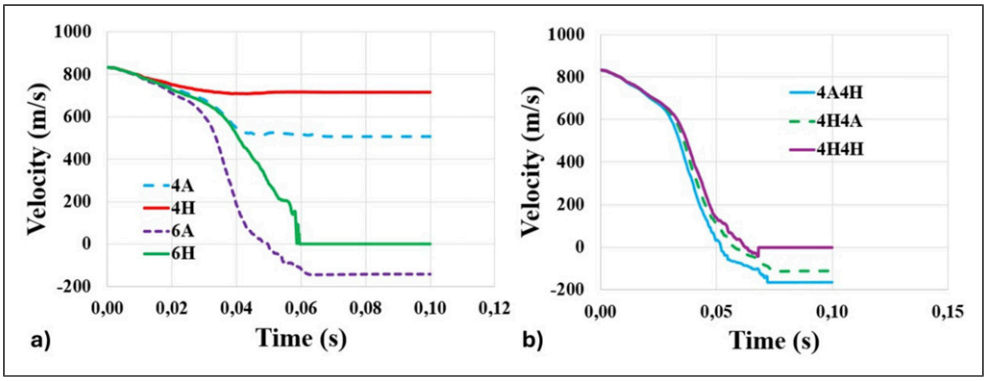

Figure 5. Projectile initial and residual numerical velocity-time graphs (a) monolithic steels; (b) double-layer armor panels.

code error at the time 0.033 ms (Figure 4(a), (b)). To mitigate this, Hourglass type 4 with a coefficient of 0.1 was implemented (Başaran et al., 2017; Deka et al., 2008). This reduced the hourglass energies for Armox 500T and Hardox 450 plates, bringing them within acceptable limits (Figure 4(c), (d)).

To model the penetration of the bullet into the armor plates, the ERODING_SURFACE_TO_SURFACE card was selected. This contact algorithm is capable of updating contact surfaces as material erodes, providing a more realistic simulation of the interaction. However, initial simulations using the standard algorithm (SOFT = 0) resulted in problematic behavior, such as surfaces penetrating each other without damage or applying excessive force that led to unrealistic damage. These issues are common when using SOFT = 0 with materials that have a large difference in bulk modulus, as shown by the penalty stiffness equation (3) (Hallquist JO., 2006):

$$k = \frac{\alpha K A^2}{V} \tag{3}$$

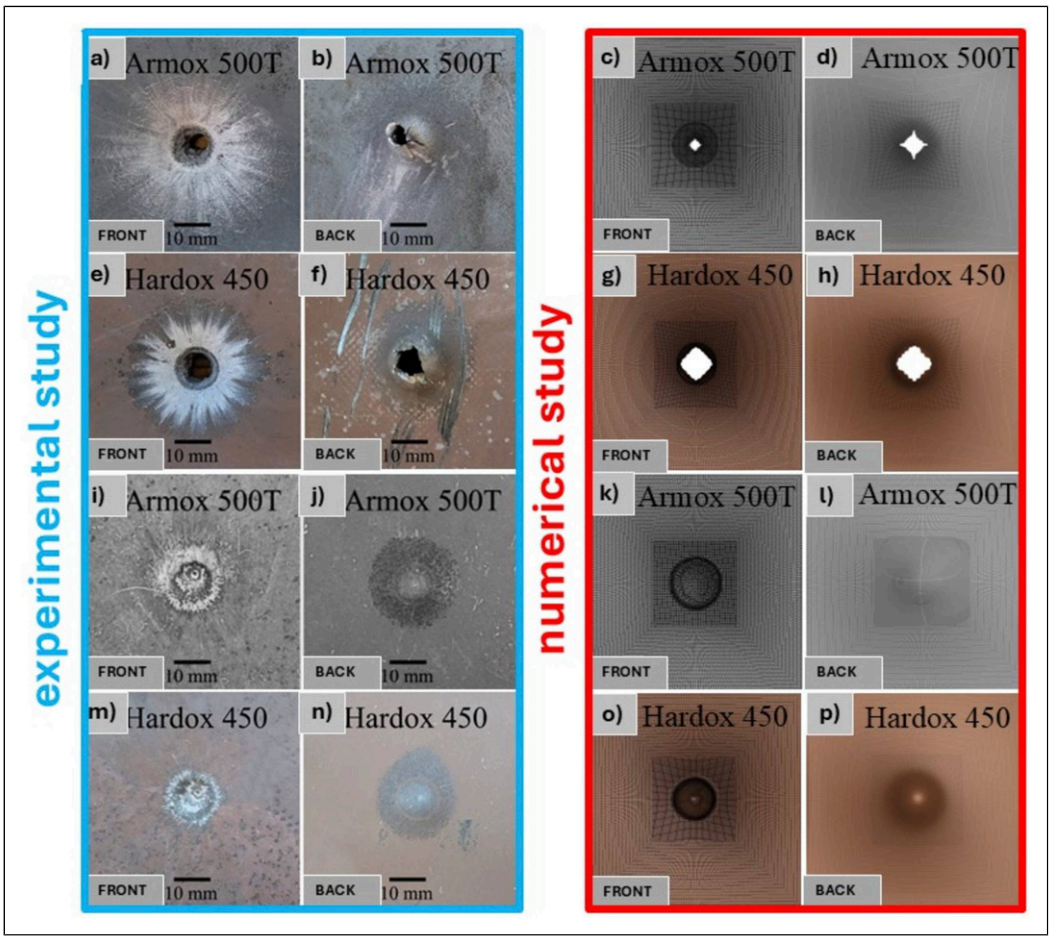

Figure 6. Damage modes of plates providing ballistic protection; (a-d) 4A; (e-h) 4H; (i-l) 6A; (m-p) 6H.

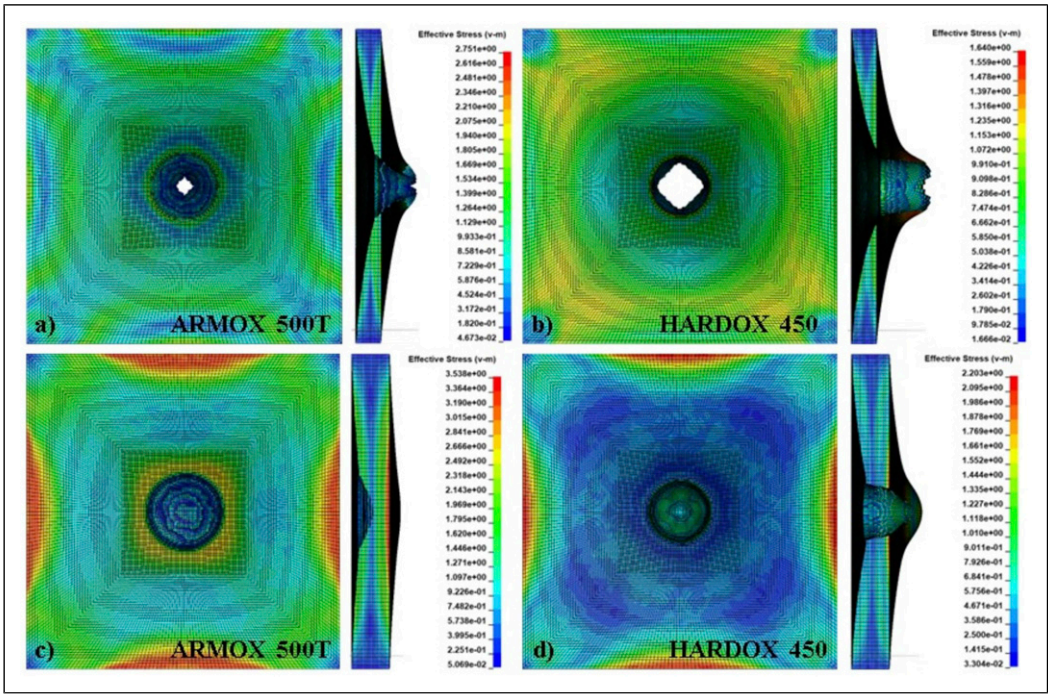

Figure 7. Von-Mises stress distribution of the layers of (a) 4A; (b) 4H; (c) 6A; (d) 6H.

Where k is the interface stiffness, K is the material bulk modulus, ρ is the penalty scale factor, A is the segment area, and V is the element's volume.

Similarly, the SOFT = 2 algorithm, while better for detecting contact surfaces, can be problematic with materials of significantly different densities. The penalty stiffness for SOFT = 2 is given by equation (4) (Hallquist JO., 2006):

$$k = 0.5\mathrm{SLSFAC}\{\mathrm{SFS\ OR\ SFM}\}\left(\frac{(\mathrm{m_1 m_2})}{(\mathrm{m_1 + m_2})}\right)\frac{1}{dtc^2} \tag{4}$$

where slsfac is the default penalty stiffness, sfs is the slave penalty stiffness factor (same equation for master). The segment masses are m_1 and m_2, and the contact time step is denoted by dtc.

To address the issues of incorrect surface detection and excessive damage, the SOFT option was specifically set to 2, which uses a pinball contact algorithm to detect segments effectively. To prevent the previously observed excess damage, the contact time-step (DTSTIF) was analytically calculated and implemented in Optional Card C. This parameter directly controls the forces and detection of contact surfaces, thereby stabilizing the interaction. Additionally, the ECDT option on the CONTROL_CONTACT card was set to 1 to block the influence of ERODING_CONTACT (Hallquist JO., 2006) on the analysis step time (Table 6).

Given the high velocity of the bullet, the MAXPAR (Maximum Parametric Coordinate Search) was increased from 1.025 to 1.12 to improve the accuracy of segment searching. The DEPTH option was set to 5 to ensure that both surface and edge contact points were properly checked.

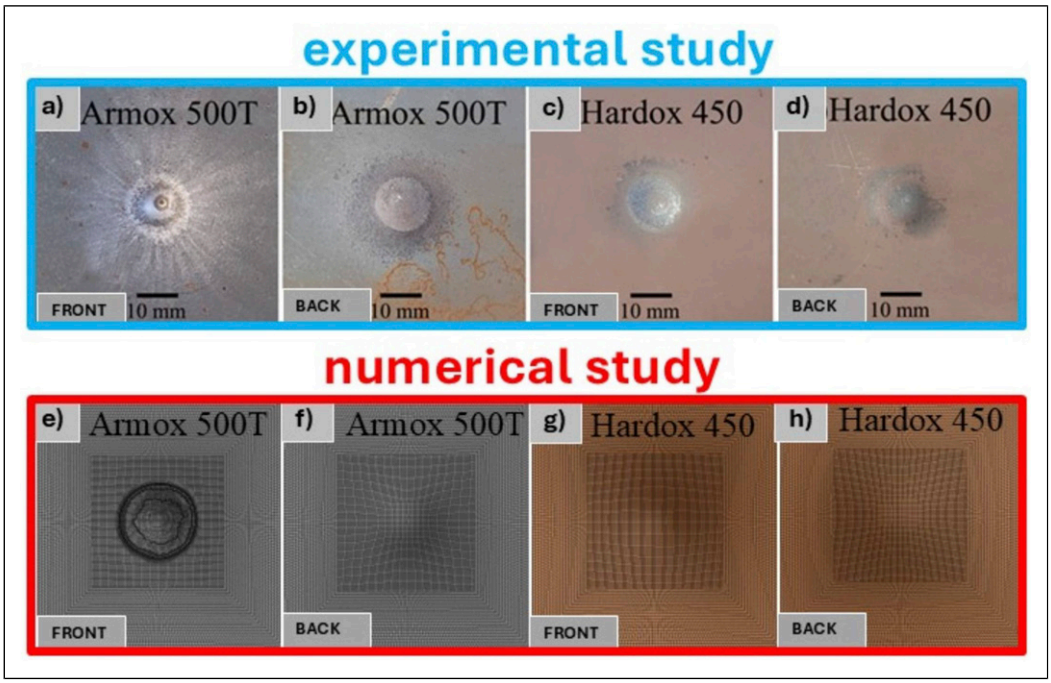

Figure 8. Damage modes of the 4A4H plate providing ballistic protection.

Discussion and results

Evaluation of experimental and numerical results of monolithic panels

First, four monolithic steel panels of identical thickness were evaluated: 4A, 4H, 6A, and 6H. As anticipated, the 4A sample with a higher hardness value had a much lower residual velocity compared to the 4H sample (Figure 5(a)). Samples 4 A and 4H both suffered from petalling damage mode (Figure 6(b), (f)). Additionally, several radial fractures, consistent with the literatüre (Showalter, 2008), formed around the hole. The bullet exit diameter of sample 4A is smaller than that of sample 4H and its geometry was determined to be non-circular. In addition, sample 4A had more and longer radial fractures than sample 4H. The rear sides of plates 6A and 6H showed that 7.62 × 51 mm FMJ failed to achieve full perforation, resulting in craters with depths of 1.10 mm and 1.92 mm, respectively. The back surface bulging damage mechanism was seen in the 6A and 6H steel samples (Figure 6(j), (n)). The back face deformation in the monolithic 6A sample was, as anticipated, less than that in the 4A sample.

Figure 6 presents the Von Mises stress distribution of the monolithic steel plates. As seen in Figure 7(a), the stress values were higher in sample 4A. The bullet penetrated in a conical shape, and the crater depth and exit hole diameter were found to be less than in sample 4H. The bullet produced a cylindrical perforation in sample 4H (Figure 7(b)). The steel plate thickness increased in samples 6A and 6H, resulting in higher stress levels (Figure 7(c), (d)). Sample 6A (Figure 7(c)) behaved more strongly than sample 6H (Figure 7(d)), with a larger crater diameter and a smaller crater depth, confirming the experimental findings.

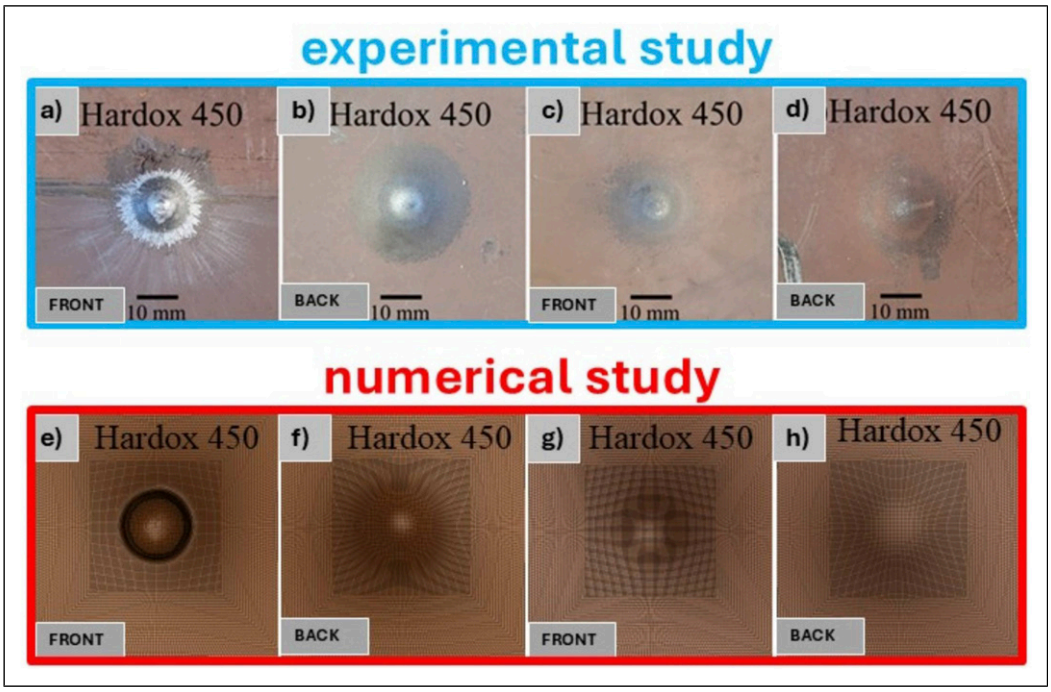

Figure 9. Damage modes of the 4H4H plate providing ballistic protection.

Evaluation of experimental and numerical results of double-layered steel panels

The behavior of double-layered steel samples applying monolithic steels was investigated since 4 mm monolithic steels failed to offer ballistic resistance. These are 4A4H, 4H4A and 4H4H double-layered steel samples with a thickness of 8 mm. Among the double-layered steels, ballistic testing of the 4H4A sample was not performed, the results were presented numerically. All double-layered steel samples absorbed the bullet's energy, with no perforation and damage resulting from bullet penetration (Figure 5(b)). As shown in Table 8, the overall back face deformation values of the 4A4H and 4H4A samples were identical, however the 4H4H sample induced greater back deformation. This result may be elucidated by the superior hardness of the Armox 500T armour steel on the front side, which forms the 4A4H sample, compared to the Hardox 450 steel23. This result is compatible with the literature (Bekci et al., 2021; Deng et al., 2024; Yilmazcoban and Doner, 2016; Yunfei et al., 2014). As both plates demonstrated ballistic protection, no complete perforation damage mode was seen. The front steel plates exhibited bulging damage (Figures 8 and 9(a), (b)), whereas the rear plates displayed smooth bulge damage (Figures 8 and 9 (c), (d)). The double-layered Armox 500T and Hardox 450 plates effectively stopped the bullet, with the frontal plate remained unperforated. The increase in performance may be attributed to the higher bending resistance of double-layered plates relative to monolithic plates, reported in the literatüre (Teng, 2008). The finite element results of double-layered steels coincide with the experimental damage conditions (Figures 8 and 9(e–h)).

Figure 9 presents the Von-Mises stress distribution results of double-layered steel samples. The 4A4H and 4H4A samples showed lower numerical values for back face signatures (Table 8) and

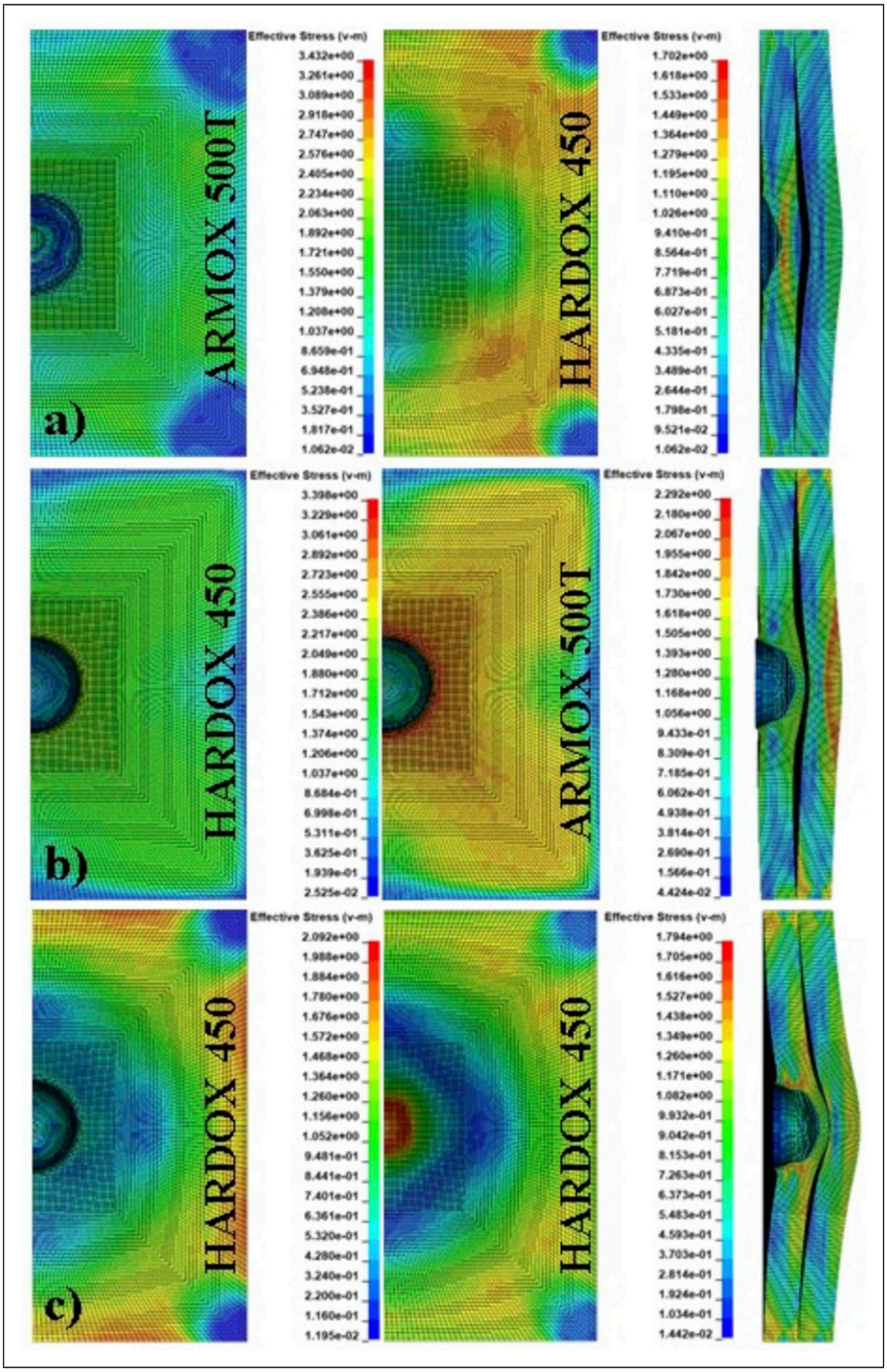

Figure 10. Von-Mises stress distribution of the layers of (a) 4A4H; (b) 4H4A; (c) 4H4H.

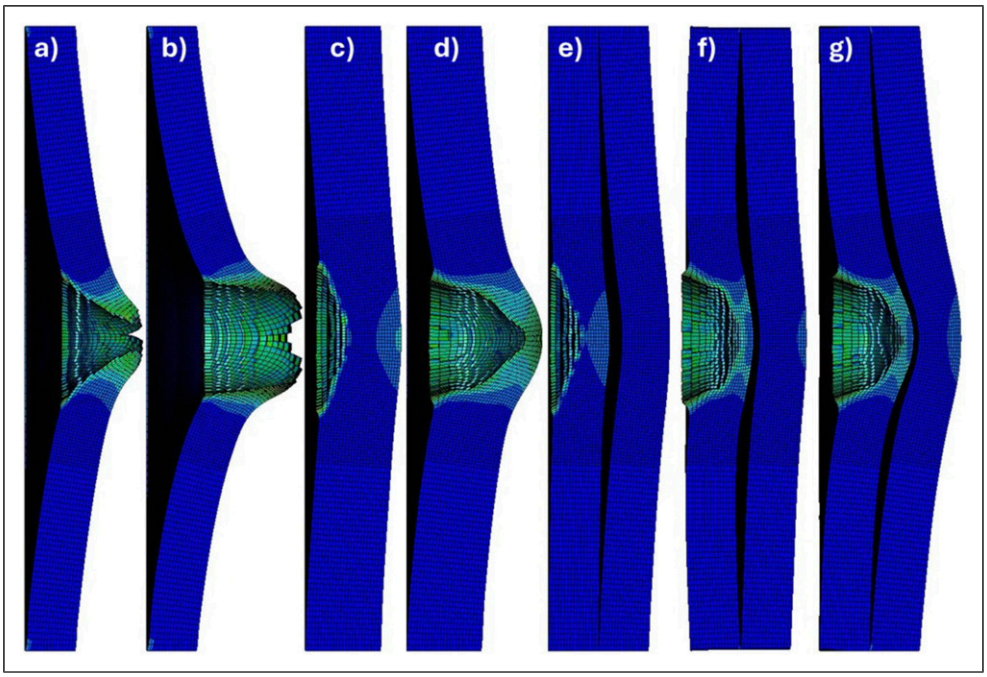

Figure 11. Effective plastic strain values in ballistic panel sections (a) 4A; (b) 4H; (c) 6A; (d) 6H; (e) 4A4H; (f) 4H4A; (g) 4H4H.

deeper bullet penetrations (Figure 10 (a–c)). The higher stresses in the edges of the 4H4H steel plate specimen result from larger deformations of the plates. This case may be attributed to the lower hardness value of Hardox 450 steel.

The effective plastic strain distributions in the cross-sections of monolithic and double-layered steel panels are given in Figure 11. Armox 500T steel suffered less plastic deformation compared to Hardox 450 steel at monolithic plate thicknesses of 4 mm and 6 mm (Figure 11 (a–d)). The analysis of double-layered samples produced identical results, demonstrating that the use of Armox 500T steel exhibited less plastic deformation (Figure 11 (e–g)).

Comparison of best samples providing ballistic protection

Monolithic 6A steel had the lowest permanent deformation value, followed by double-layer steel samples. However, the areal weights of double-layer steel samples are higher. The areal density of the 6A sample is 7.83 kg/m^2, the 4A4H sample is 7.98 kg/m^2. It was found that the 4A4H sample

Table 7. Specific energy absorption (SEA) of the best samples.

Configuration	SEA (Joule/kg)	Mass (kg)	Thickness (mm)
6A	244.54	3.19	6.00
4A4H	209.34	4.08	8.00

Table 8. Comparison between the experimental and simulation results.

Sample code	Muzzle velocity (m/s)	FEM residual speed (m/s)	Full perforation	Sample thickness (mm)	Back face deformation			
					Experiment (mm)		Simulation (mm)	
4A	837 ± 3.08	544	Yes	4	–		–	
4H		774	Yes	4	–		–	
6A		–	No	6	1.10		1.12	
6H		–	No	6	1.92		2.98	
					Front	Back	Front	Back
4A4H		–	No	8	0.93	1.47	1.24	1.95
4H4A		–	No	8			1.47	1.61
4H4H		–	No	8	3.09	2.79	4.11	3.72

was 20.15% heavier than the 6A sample, but both of the samples were with regard to the same cost. There are differences in damage mechanisms among samples that absorb all bullet energy. The bulge damage in sample 6A was less severe than in samples 4A4H, 4H4A and 4H4H. Additionally, the specific energy absorptions of the best samples are given in (Table 7).

As seen in Table 8, the 6A design is the thinnest choice, however it cannot absorb a lot of impact energy and can be regarded at the limit of ballistic resistance. The 4A4H sample also has no ability to absorb further impact energy. It can be concluded that monolithic and double-layered steel specimens exhibit superior experimental performance; however, further analysis using finite element analysis reveals that their energy absorption capacity is at its limit. The 4A4H sample has a 14.39% lower specific energy absorption (SEA) compared to the 6A sample.

Conclusions

The ballistic resistance of seven different armour combinations four made of monolithic steel and three made of double-layered steel was evaluated numerically and experimentally. During the ballistic testing, the armour combinations applied to resist 7.62 mm full metal jacket bullet impacts had a muzzle velocity of 837 ± 3.08 m/s. Ballistic testing was performed on the configurations in accordance with NIJ STD-0101.08 Level III-A.

The following conclusions can be made from this research:

- Monolithic steels with a thickness of 6 mm experienced bulging damage and showed less back face deformation compared to double-layer steels.
- 6 mm of Armox 500T steel is the most costly test specimen, offering ballistic protection.
- Although double-layer steels provide ballistic protection and could be an alternative to monolithic steels, monolithic steel exhibits more benefits over double-layer steels with regard to cost and weight.
- In 4 mm monolithic steel plates with full perforation, Armox 500T and Hardox450 steels produced different damage zone in terms of radial crack and hole geometry.
- In the double-layered steel samples, primarily bulging failure mechanisms were observed. The use of the Armox 500T as the face plate resulted in reduced back face signature and enhanced ballistic resistance of double-layered steels.

- As a result of nonlinear finite element analysis, the damage mechanisms were consistent with the experimental results.
- Future research aims to analyze the multi-layered armor steel configurations proposed in this work for its ballistic resistance against larger caliber and armour piercing (AP) bullets.

Acknowledgments

The authors would like to thank ZSR Inc. (Balıkesir, Turkey) for allowing ballistic testing using their outdoor shooting ranges. The authors would like to thank "Numesys, Türkiye", the solution partner of Dr. Yılmazçoban's "IKY Research Group", for their support with Ansys and LS-DYNA.

ORCID iD

Fatih Balıkoğlu https://orcid.org/0000-0003-3836-5569

Funding

The authors received no financial support for the research, authorship, and/or publication of this article.

Declaration of conflicting interests

The authors declared no potential conflicts of interest with respect to the research, authorship, and/or publication of this article.

Data Availability Statement

The authors confirm that the data supporting the results of this study are available within the article.

References

Acar D, Canpolat BH and Cora ÖN (2024) Ballistic performances of Ramor 500, Armox advance and Hardox 450 steels under monolithic, double-layered, and perforated conditions. *Engineering Science and Technology, an International Journal* 51: 101653.

Armox 500T General Product Description. (2016). SSAB.

Başaran G and Gürses E (2017) Numerical study of high velocity impact response of vehicle armor combination using LS DYNA. In: *11th European LS-DYNA Conference*, Salzburg, Austria, Copyright by DYNAmore GmbH.

Bekci ML, Canpolat BH, Usta E, et al. (2021) Ballistic performances of Ramor 500 and Ramor 550 armor steels at mono and bilayered plate configurations. *Engineering Science and Technology, an International Journal* 24(4): 990–995.

Børvik T, Hopperstad OS, Berstad T, et al. (2002a) Perforation of 12mm thick steel plates by 20mm diameter projectiles with flat, hemispherical and conical noses. *International Journal of Impact Engineering* 27(1): 37–64.

Børvik T, Langseth M, Hopperstad OS, et al. (2002b) Perforation of 12mm thick steel plates by 20mm diameter projectiles with flat, hemispherical and conical noses. *International Journal of Impact Engineering* 27(1): 19–35.

Børvik T, Hopperstad OS, Langseth M, et al. (2003) Effect of target thickness in blunt projectile penetration of Weldox 460 E steel plates. *International Journal of Impact Engineering* 28(4): 413–464.

Deka LJ, Bartus SD and Vaidya UK (2008) Damage evolution and energy absorption of E-glass/polypropylene laminates subjected to ballistic impact. *Journal of Materials Science* 43(13): 4399–4410.

Deng Y, Yang B, Wei G, et al. (2024) Ballistic performance of double-layered plates Q235 and 45 steel subjected to impact by projectiles of middle strength. *Mechanics of Advanced Materials and Structures* 31(26): 8648–8661.

Hallquist JO (2006). *LS-DYNA Theory Manual*.

İbış MÖ, Kahraman Y and Genel K (2023) Effect of adhesive on ballistic performance of multi-layered steel. *International Journal of Impact Engineering* 176: 104559.

Johnson GR (1983) A constitutive model and data for metals subjected to large strains, high strain rates and high temperatures. In: *Proceedings of the 7th International Symposium on Ballistics*, Netherlands. pp. 541-547. The Hague.

Kasilingam S, Iqbal MA and Senthil R (2019) Influence of impactor nature, mass, size and shape on ballistic resistance of mild steel and Armox 500 T steel. *International Journal of Protective Structures* 10(2): 174–197.

Miloradovic N, Nestorovic K, Trifkovic D, et al. (2025) Experimental and numerical examination of perforation of Armox 500t high hardness steel plate by projectiles of small arms ammunition.

Morghode DS, Thakur DG, Salunkhe S, et al. (2024a) Analysis of the thickness of layered armor to provide protection against 7.62 mm ball projectiles using experimental and numerical methods. *Frontiers of Mechanical Engineering* 10: 1419210.

Morghode DS, Thakur DG, Salunkhe S, et al. (2024b) Numerical study on the optimized thickness of layer configuration against the 7.62 APM2 projectile. *Frontiers of Mechanical Engineering* 10: 1322640.

Mubashar A, Uddin E, Anwar S, et al. (2019) Ballistic response of 12.7 mm armour piercing projectile against perforated armour developed from structural steel. *Proceedings of the Institution of Mechanical Engineers, Part L: Journal of Materials: Design and Applications* 233(10): 1993–2005.

Mulabagal P, Kumaraswamy A, Dewangan MK, et al. (2024) Comparative study of effect of fragment nose shapes on damage characteristics of thin target plate in ballistic applications. *Proceedings of the Institution of Mechanical Engineers - Part C: Journal of Mechanical Engineering Science* 238(19): 9660–9671.

NIJ 0108.01 (1985) Ballistic resistant protective materials.

Orlov MY and Fazylov TV (2022) Research of the Behaviour of multi-layered Steel Targets Impacted by High-Velocity Projectiles. In: Orlov M.Y. and Visakh P. M. (eds). *Behavior of Materials under Impact, Explosion, High Pressures and Dynamic Strain Rates. Advanced Structured Materials*. Switzerland: AG, Springer, 145–167.

Orlov MY, Orlova YN and Fazylov TV (2024) Numerical simulation of behavior of multi-layered metal targets impacted by high-velocity striker. *Proceedings of the Institution of Mechanical Engineers - Part C: Journal of Mechanical Engineering Science* 238(10): 4757–4767.

Paman A, Sukumar G, Ramakrishna B, et al. (2020) An optimization scheme for a multilayer armour module against 7.62 mm armour piercing projectile. *International Journal of Protective Structures* 11(2): 185–208.

Qiang L, Zhang R, Zhao C, et al. (2022) Multiple ballistic impacts of thin metallic plates: numerical simulation. *Proceedings of the Institution of Mechanical Engineers - Part C: Journal of Mechanical Engineering Science* 236(14): 7962–7973.

Ranaweera P, Weerasinghe D, Fernando P, et al. (2020) Ballistic performance of multi-metal systems. *International Journal of Protective Structures* 11(3): 379–410.

Saleh M (2016) Analysis of the residual stress in ARMOX 500T armour steel and numerical study of the resultant ballistic performance. In: Holden T. M., Muránsky O. and Edwards L. (eds). *10th International Conference on Residual Stresses*. Sydney, Australia, 3-7 July 2016, USA: Materials Research Forum LLC Publishing, 437–442.

Senthil K and Iqbal MA (2021) Prediction of superior target layer configuration of armour steel, mild steel and aluminium 7075-T651 alloy against 7.62 AP projectile. *Structures* 29: 2106–2119.

Senthil K, Iqbal MA, Bhattacharjee D, et al. (2015) Ballistic resistance of Armox 500T steel plates against 7.62 API projectiles. In: 3rd International Conference on Protective Structures, Callaghan, NSW, 2015, 3–6.

Showalter DD ,(2008) Ballistic testing of SSAB ultra-high-hardness steel for armor applications.

Sirigiri VKR, Gudiga VY, Gattu US, et al. (2022) A review on Johnson cook material model. *Materials Today: Proceedings* 62: 3450–3456.

Teng XWT, Wierzbicki T and Huang M (2008) Ballistic resistance of double-layered armor plates. *International Journal of Impact Engineering* 35: 870–884.

Ulewicz R, Mazur M and Bokůvka O (2013) Structure and mechanical properties of fine-grained steels. *Periodica Polytechnica Transportation Engineering* 41(2): 111–115.

Yilmazcoban IK and Doner S (2016) Ballistic protection evaluation of sequencing the composite material sandwich panels for the reliable combination of armor layers. *Acta Physica Polonica A* 130(1): 342–346.

Yunfei D, Wei Z, Yonggang Y, et al. (2014) Experimental investigation on the ballistic performance of double-layered plates subjected to impact by projectile of high strength. *International Journal of Impact Engineering* 70: 38–49.